Study of the One-Dimensional Ising Model Using Computational Simulations

Sanchez-Toril Bastrygina, Andrés

[a]*Higher Technical School of Telecommunication Engineering, Valencia,*

Abstract

In this article, we derive analytical expressions for the average energy, magnetization, magnetic susceptibility, and specific heat per particle as functions of temperature, based on the hypotheses of the model proposed by Ernest Ising. Subsequently, these calculations are validated by simulating a spin chain computationally, considering cases where the external magnetic field is either zero or takes positive values. Finally, the obtained results are discussed, and pertinent conclusions are presented, along with a general understanding of the system's behavior.

1. Context and Introduction

The Ising model is a problem originally formulated by physicist Wilhelm Lenz in 1920 and solved by his student Ernest Ising in his 1924 thesis [1]. Its significance lies in being one of the first models solved exactly for an interacting system, enabling a description of ferromagnetism and phase transitions. The exact solution for the two-dimensional case was obtained by Lars Onsager in 1944. Today, its importance transcends statistical physics and has applications in other fields, such as biology.

2. Analytical Solution

The one-dimensional Ising model consists of a linear spin chain (represented as $\sigma_i = \pm 1$), where periodic boundary conditions are applied after N elements ($\sigma_{i+N} = \sigma_i$). In one dimension, this approximation is equivalent to a ring. Starting from the Hamiltonian:

$$H = -J \sum_{i=1}^{N} \sigma_i \sigma_{i+1} - B \sum_{i=1}^{N} \sigma_i \tag{1}$$

where J is a coupling constant and B is the product μH, with H being the applied external magnetic field, we arrive at the following expression after applying the boundary conditions:

$$H = -J \sum_{i=1}^{N} \sigma_i \sigma_{i+1} - \frac{B}{2} \sum_{i=1}^{N} (\sigma_i + \sigma_{i+1}) \tag{2}$$

Considering the canonical ensemble (the number of spins does not vary), the partition function can be calculated as $Z = \sum_{\sigma_i} e^{-\beta H}$. This expression can be reformulated as:

$$Z_N = \sum_{\sigma_i} e^{\sum_{i=1}^{N} K \sigma_i \sigma_{i+1} + b \frac{\sigma_i + \sigma_{i+1}}{2}} \tag{3}$$

where K is the product βJ and b is the product βB. The summation in the exponent of the exponential can be cyclically factored, allowing us to rewrite the partition function as a product of terms defined as:

$$\mathbb{T}_{\sigma\sigma'} = e^{K\sigma\sigma' + b\frac{\sigma+\sigma'}{2}} \tag{4}$$

which can be considered the elements of a matrix $\mathbb{T}$, called the transfer matrix. Using this, we arrive at the following expression for the partition function:

$$Z_N = \sum_{\sigma_i} \mathbb{T}_{\sigma_1\sigma_2} \mathbb{T}_{\sigma_2\sigma_3} ... \mathbb{T}_{\sigma_{N-1}\sigma_N} \mathbb{T}_{\sigma_N\sigma_1} = \sum_{\sigma_1 = \pm 1} (\mathbb{T}^N)_{\sigma_1\sigma_1} \tag{5}$$

This is equivalent to $Z_n = Tr\{\mathbb{T}^N\}$, and since $\mathbb{T}$ is a symmetric matrix, its eigenvalues are real. Therefore, we can rewrite Z_n as $Z_n = \lambda_+^N + \lambda_-^N$. These eigenvalues are given as follows [2]:

$$\lambda_\pm = e^K \left[\cosh(b) \pm \sqrt{\sinh^2(b) + e^{-4K}} \right] \tag{6}$$

Knowing that the value of λ_+ is larger than that of λ_-, we can refactor the expression for Z_n as $Z_n = \lambda_+^N (1 + (\lambda_-/\lambda_+)^N)$, and therefore, in the thermodynamic limit ($N \to \infty$), we can approximate $(\ln Z_N)/N \approx \ln \lambda_+$.

2.1. Average Magnetization

Magnetization is defined as [3]:

$$M = -\left(\frac{\partial F}{\partial B} \right) \tag{7}$$

where F is the Helmholtz free energy, defined as $F = -\ln(Z_N)/\beta$, or equivalently:

$$M = \left(\frac{\partial \ln Z_N}{\partial b} \right) \tag{8}$$

Using the thermodynamic limit approximation calculated earlier, we arrive at the following expression for magnetization:

$$M \approx N \left(\frac{\partial \ln \lambda_+}{\partial b} \right) = \frac{N \sinh(b)}{\sqrt{\sinh^2(b) + e^{-4K}}} \tag{9}$$

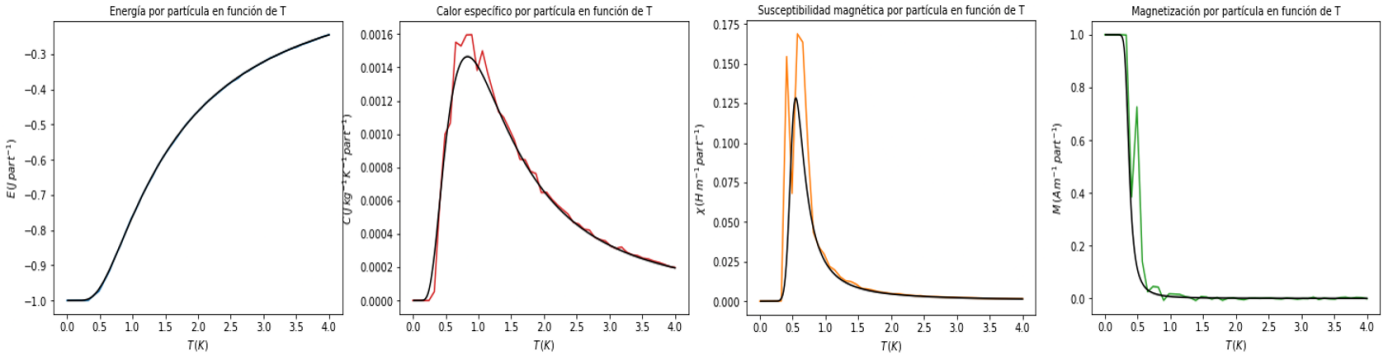

Figure 1: Expressions for energy, specific heat, magnetic susceptibility, and magnetization as functions of temperature per particle, determined through computational methods (colored) and analytically (black) at zero external field, using 300 particles and 7.5×10^5 iterations.

We define the magnetization per spin, $\langle \sigma_i \rangle$, as $\langle \sigma_i \rangle = \langle M \rangle / N$. For the case where the external field is zero (which implies $b = 0$), $\langle \sigma_i \rangle$ sharply tends to 0 for $T > 0$, which can be interpreted as a phase transition with $T_c = 0$ for the one-dimensional case. The function takes a value of 1 when $T = 0$.

2.2. Average Energy

Energy is defined as [3]:

$$E = -\left(\frac{\partial \ln Z_N}{\partial \beta}\right) \approx -N\left(\frac{\partial \ln \lambda_+}{\partial \beta}\right) \tag{10}$$

The second equivalence is the thermodynamic limit approximation. Knowing the expression for λ_+, we can calculate this expression in the given limit. Due to its length, it is omitted in this document but can be viewed in the code provided as an appendix. For the case where the external field is zero ($b = 0$), we can simplify the above expression to:

$$E_{(H=0)} = \frac{NJ\left(1 - e^{4K}\sqrt{e^{-4K}}\right)}{\left(1 + e^{4K}\sqrt{e^{-4K}}\right)} \tag{11}$$

2.3. Specific Heat

Specific heat is defined as [3]:

$$C = -\left(\frac{\partial E}{\partial T}\right) \tag{12}$$

Using the chain rule, we can rewrite the derivative as:

$$C = \frac{J}{k_B T}\left(\frac{\partial E}{\partial K}\right) \tag{13}$$

For the case where the external magnetic field is zero, knowing the expression for energy in this case, we obtain the following result for the derivative:

$$C_{(H=0)} = \frac{4NK^2 k_b e^{-4K}\sqrt{e^{-4K}}}{\left(e^{-4K}\sqrt{e^{-4K}} + 1\right)^2} \tag{14}$$

As with the energy in the case where the external magnetic field is not zero, the specific heat expression for that case is too extensive to be written in the article but can be viewed in the appendix code. To ensure both analytical expressions align with the subsequent numerical analysis, it was necessary to divide the expressions by N^2 since the computational calculation uses an average for its determination.

2.4. Magnetic Susceptibility

Magnetic susceptibility is defined as [3]:

$$\chi = -\left(\frac{\partial M}{\partial B}\right) \tag{15}$$

Knowing the value of magnetization (9), we can calculate this derivative, leading to the following analytical expression:

$$\chi = \frac{N\beta \cosh(b)\, e^{4K}\sqrt{\sinh^2(b) + e^{-4K}}}{e^{8K}\sinh^4(b) + 2e^{4K}\sinh^2(b) + 1} \tag{16}$$

Similar to the specific heat, to compare this expression to the one obtained through numerical calculations, it was necessary to divide it by a factor of N^2 since computational calculations use an average for their determination.

3. Computational Simulations

To simulate a chain of spins, we used the Metropolis-Hastings algorithm [4]. This method starts with a random initial configuration ($\sigma_i = \pm 1$) and modifies the value of a randomly selected spin in each iteration. After recalculating the energy variation resulting from this change, if $\Delta E \leq 0$, the change is accepted. If $\Delta E > 0$, the change is accepted with a probability $p = e^{-\beta \Delta E}$. These iterations are repeated sufficiently to allow the system to explore a significant portion of its associated phase space. In our study, we used a total of $N = 300$ particles, for which the Metropolis-Hastings method performed a total of $2500 \cdot N$ iterations. The numerical plots were computed for a magnetic induction value of $B = 1.5$.

3.1. Average Magnetization

The system's magnetization can be computationally estimated by averaging the sums of the lists containing the spin chain values after each iteration of the method. This idea can be synthesized in the following expression:

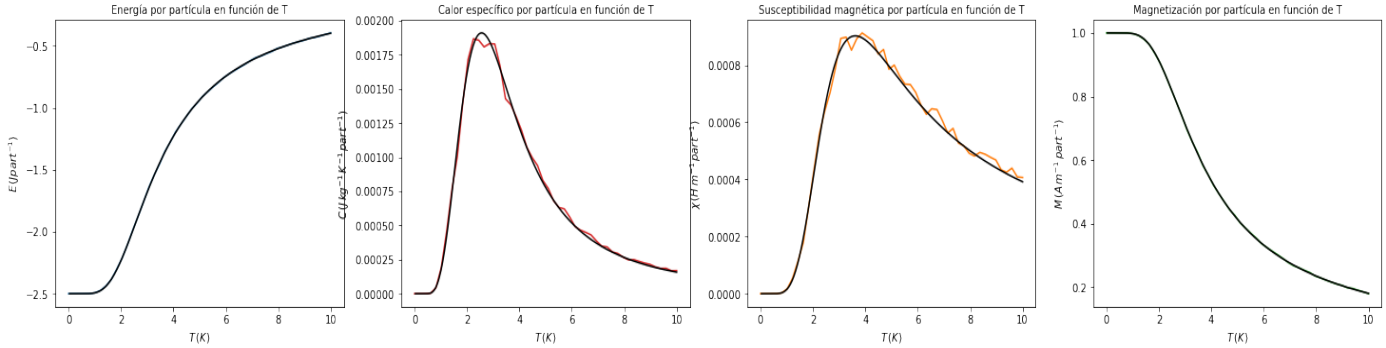

Figure 2: Expressions for energy, specific heat, magnetic susceptibility, and magnetization as functions of temperature per particle, determined through computational methods (colored) and analytically (black), with magnetic field intensity $B = 1.5\,T$, using 300 particles and 7.5×10^5 iterations.

$$\overline{M} = \frac{1}{n}\sum_{K=1}^{n}\sum_{i=1}^{N}\sigma_i^{(K)} \tag{17}$$

Here, N is the total number of spins, n is the number of method iterations, $K = 1, 2, ..., n$ is the number of configurations sampled, and $\sigma_i^{(K)}$ is the value of spin i in configuration K. The calculation is the same for cases with zero or positive external fields. In both cases, the algorithm was applied in a loop, with a range of equally spaced temperature values passed as parameters to the program. As a result, an estimation of magnetization as a function of temperature was obtained (see fig. 1, fig. 2).

3.2. Average Energy

The system's average energy can be estimated as the mean of the Hamiltonians. Using expression (1) derived earlier, for the case of a null external magnetic field ($B = 0$), the Hamiltonian expression can be computed as:

$$H_{(H=0)}^{(K)} = -J\sum_{i=1}^{N}\sigma_i^{(K)}\sigma_{i+1}^{(K)} \tag{18}$$

Consequently, the average energy expression can be written as:

$$\overline{E} = \frac{1}{n}\sum_{K=1}^{n}H_{(H=0)}^{(K)} \tag{19}$$

Similar to magnetization, by calculating the system's average energy with different initial temperature values, an approximation of the average energy curve as a function of temperature can be determined (see fig. 1).
For cases where there is a non-zero external magnetic field, the Hamiltonian to average is given by expression (1), but this time including the term $-B\sum_{i=1}^{N}\sigma_i^{(k)}$. Its temperature dependence was also computed numerically (see fig. 2).

3.3. Specific Heat

To compute specific heat numerically, we need to calculate the fluctuation of the average energy and divide the result by k_BT^2, where k_B is the Boltzmann constant. For this, it is necessary to obtain the average of the squared energy values, which can be calculated by averaging the squared Hamiltonians after each iteration. First, considering a null external field, the specific heat was computed as:

$$\overline{C} = \frac{1}{k_BT^2}\left[\left(\frac{1}{n}\sum_{K=1}^{n}H_{(H=0)}^{(K)\,2}\right) - \left(\frac{1}{n}\sum_{K=1}^{n}H_{(H=0)}^{(K)}\right)^2\right] \tag{20}$$

As with the two previous parameters, its temperature dependence was computed (see fig. 1).
For cases where the external field is non-zero, the specific heat was calculated using the same method but with Hamiltonians including the term $-B\sum_{i=1}^{N}\sigma_i^{(k)}$. A numerical approximation of the analytical function derived in the first section was also obtained (see fig. 2).

3.4. Magnetic Susceptibility

In this case, it is again necessary to calculate the fluctuation of a variable, in this case, the average magnetization. Similar to specific heat, the result must be divided by k_BT. The mean value of the square of magnetization is obtained by averaging the square of the sum of spins in each configuration after every iteration. The resulting expression can be written as:

$$\overline{\chi} = \frac{1}{k_BT}\left[\frac{1}{n}\sum_{K=1}^{n}\left(\sum_{i=1}^{N}\sigma_i^{(K)}\right)^2 - \left(\frac{1}{n}\sum_{K=1}^{n}\sum_{i=1}^{N}\sigma_i^{(K)}\right)^2\right] \tag{21}$$

The method is identical for both cases of zero and non-zero external magnetic fields. Numerical approximations of their respective temperature dependencies have been determined (see fig. 1, fig. 2).

4. Discussion of Results

After implementing the Metropolis-Hastings algorithm for solving the 1D Ising model, obtaining the analytical results, and comparing the two, we now proceed to discuss the results obtained from the graphs.

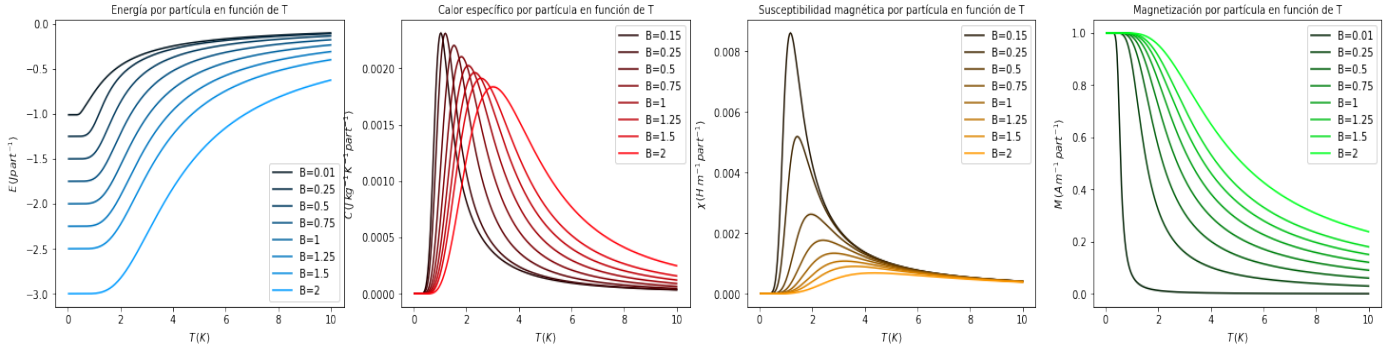

Figure 3: Variations in energy, specific heat, magnetic susceptibility, and magnetization dependencies on temperature per particle for different values of B. $N = 300$ was used.

4.1. Results Without External Field

4.1.1. Average Energy

As seen in the graph, energy increases as the system temperature rises. Both the analytical and numerical approaches exhibit identical system behavior, matching almost perfectly across all values. The increase in energy with temperature is intuitive, as higher temperatures correspond to greater atomic motion, generating more energy in the system.

From the Metropolis algorithm's perspective, the probability of accepting a change increases with temperature, making it easier to accept changes. Consequently, the energy tends towards equilibrium, with spins constantly fluctuating between +1 and -1. At equilibrium, the average energy per particle approaches zero. This is logical since energy depends on the spin's sign, and at infinite temperature, approximately half of the spins will be +1 and the other half -1, resulting in energy tending to zero as temperature increases.

Finally, we observe that energy seems constant at low temperatures. Physically, this occurs because spins exhibit minimal movement at low temperatures. From the algorithm's perspective, this is because the probability of accepting a change is nearly zero at low temperatures.

4.1.2. Magnetization

Magnetization exhibits a sharp drop at a certain temperature, called the critical or Curie temperature [5]. This temperature marks the phase transition from ferromagnetic to paramagnetic. Theoretically, in one dimension, the critical temperature is 0, so this phase transition would not occur. However, in our calculations, this critical temperature is found between 0.5 and 1, a minor shift that does not significantly affect the final result. Qualitatively, magnetization tends to zero, aligning with Curie's law of paramagnetism, which inversely relates magnetization to temperature, approaching zero at high temperatures. This law is expressed as:

$$\vec{M} = \chi \vec{H} = \frac{C}{T}\vec{H} \tag{22}$$

where C is Curie's constant, $\vec{H}$ is the external magnetic field, and T is temperature.

4.1.3. Specific Heat

Specific heat represents the variation of average energy with temperature. In the graph, specific heat peaks precisely at the critical temperature, where the system undergoes a phase transition. At this temperature, the variation in average energy per particle is maximal because the probability of a change occurring or not is equally likely. Thus, the graph shows significant peaks and fluctuations in the critical temperature region.

4.1.4. Magnetic Susceptibility

Magnetic susceptibility behaves similarly to specific heat. This parameter indicates how susceptible a material is to magnetization. Since it is calculated based on magnetization fluctuations, it peaks where magnetization begins to decay, i.e., at the phase transition. This makes sense because magnetization transitions from a peak to a value approaching zero, aligning with Curie's law. Algorithmically, this is the point where the probabilities of accepting or rejecting changes are nearly equal, making fluctuations more significant. At higher temperatures, within the paramagnetic region, susceptibility becomes small and positive, consistent with Curie's law and paramagnetic material properties.

4.2. Results With External Field

4.2.1. Average Energy

The system's behavior is identical to the case without an external field. However, as seen in the graph, the initial energy is greater in absolute value with an external field. This is because the spins interact with the field, increasing their internal energy as they align with it. Additionally, temperature starts to increase only at higher values compared to the zero-field case because each spin's internal field makes movement more challenging as they influence each other to maintain alignment. From the algorithm's perspective, the increased energy results in greater energy increments, reducing the probability of accepting changes until sufficiently high temperatures are reached.

4.2.2. Magnetization

Adding a magnetic field makes it harder to misalign the spins due to their mutual influence. Thus, higher temperatures are required to transition from ferromagnetic to paramagnetic, as

increased energy causes greater motion, eventually misaligning the spins. Additionally, the drop in magnetization is slower. Comparing the fourth graph in figure 2 with figure 1, we see that magnetization approaches zero at a higher temperature, indicating that the critical temperature is higher with a magnetic field. From the algorithm's perspective, adding a field increases energy increments, decreasing the probability of accepting changes, which explains the slower decline in magnetization.

4.2.3. Specific Heat

With the addition of a magnetic field, higher temperatures are required to reach the specific heat maximum. This occurs because the energy difference is greater with a field than without, so the maximum specific heat value is higher. This peak coincides with the critical temperature region, marking the phase transition.

4.2.4. Magnetic Susceptibility

Adding a magnetic field raises the critical temperature, shifting the peak of magnetic susceptibility. The maximum susceptibility value is lower with a field than without, as the material is less susceptible to further magnetization when already magnetized. As the field strength increases, susceptibility decreases. Algorithmically, susceptibility is inversely proportional to $k_B T$, so increasing the temperature for the phase transition reduces its value.

5. System Behavior Analysis

This section explores how varying parameters affect results, considering both analytical curves and numerical outcomes.

5.1. External Magnetic Field Variation

The discussed quantities were graphed for different external field values (see fig. 3).

Starting with energy, we observe that higher external magnetic fields result in greater initial absolute energy, as the field contributes energy to the spins. Moreover, energy increases more slowly at higher fields because the probability of accepting changes decreases unless the temperature is sufficiently high. Physically, spins are more constrained by the internal field, requiring higher temperatures to reach equilibrium at zero energy. Specific heat behaves similarly across different magnetic fields, with only the maximum point shifting as the critical temperature increases. The peaks are lower at higher fields because energy fluctuations occur at higher temperatures, and specific heat is inversely proportional to temperature squared.

Magnetic susceptibility peaks decrease as the field increases, as higher fields reduce the material's capacity for additional magnetization. Algorithmically, magnetization fluctuations are less pronounced at higher fields, resulting in less prominent peaks. Qualitatively, the behavior is consistent across cases, with susceptibility tending to zero at high temperatures, following Curie's law.

Finally, magnetization follows expected behavior. At low fields, it quickly approaches zero with a steep slope, consistent with the 1D Ising model where the critical temperature is zero. As the field increases, magnetization declines more gradually as the critical temperature shifts, making spin misalignment more challenging due to mutual influences.

5.2. Variation in the Number of Simulated Particles

The two numerical graphs that exhibit the greatest deviation from their analytical values are the specific heat and magnetic susceptibility. Different trends, both numerical and analytical, have been plotted for varying numbers of particles (see fig. 4, 5). It is worth noting, as mentioned in the first section, that the analytical expressions for C and χ were divided by a factor of N. Thus, the number of particles becomes a parameter in the analytical function, making it non-unique and dependent on the N used in the calculations.

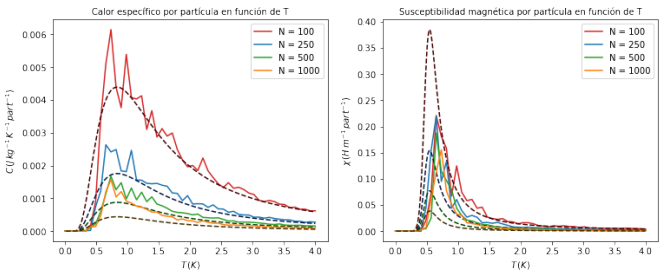

Figure 4: Analytical trends and their respective numerical approximations for specific heat and magnetic susceptibility per particle, for different numbers of simulated particles. All simulations used $300 \times N$ iterations.

For the case of a null external field (see fig. 4), it is evident that a significant number of iterations are required for the simulated graph trend to match the numerical one. For specific heat, the required order of iterations can be estimated as N^2, as only the graphs for 250 and 100 particles provide a good approximation to their analytical trends when $300 \times N$ iterations are used. For magnetic susceptibility, the required iterations exceed N^2, as even the 100-particle graph does not provide an adequate approximation. On the other hand, increasing the number of particles aids in smoothing the computed curve, reducing pronounced fluctuations. However, as shown, increasing the number of particles is detrimental to achieving a good approximation unless this increase is accompanied by a significantly higher number of iterations.

However, as seen in the figure plotting dependencies as a function of particle number with an external field (see fig. 5), convergence to analytical trends is significantly better than for the case without an external field, both for C and χ. In this case, we can again deduce that a higher number of particles results in smoother computed curves. However, it is not necessary to use an exorbitant number of iterations for these curves to resemble their corresponding analytical counterparts.

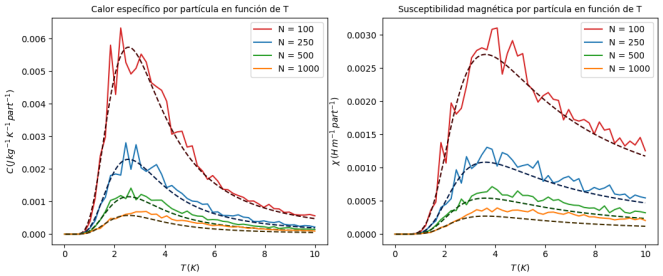

Figure 5: Analytical trends and their respective numerical approximations for specific heat and magnetic susceptibility per particle, for different numbers of simulated particles with a magnetic field intensity of $B = 1.5$. All simulations used $300 \times N$ iterations.

6. Conclusions

As demonstrated in the computational simulations section, the Metropolis algorithm is an effective method for approximating the Ising model. However, it becomes inefficient at low temperatures as the system approaches the critical temperature, leading to oscillations when calculating results.

Although the critical temperature is theoretically located at zero, the graphs show that the maximum fluctuations and the abrupt drop in magnetization occur at a slightly higher temperature. The physical rationale for the trends in the various quantities has been thoroughly discussed in the results discussion section.

Moreover, when plotting results, it has been concluded that beyond a certain number of particles, it is more critical to increase the number of steps than the number of particles to achieve good approximations.

References

[1] Ernst Ising. Beitrag zur theorie des ferromagnetismus - zeitschrift für physik a hadrons and nuclei, Feb 1925.

[2] J. Ricardo Arias-Gonzalez. Apuntes de física estadística, tema 6: Sistemas con interacción. 2023.

[3] Paul D. Beale R.K. Pathria. *Statistical Mechanics*. Katey Birtcher, 4 edition, 2022.

[4] W. K. Hastings. Monte Carlo sampling methods using Markov chains and their applications. *Biometrika*, 57(1):97–109, 04 1970.

[5] Nicola A. Spaldin. *Magnetic Materials: Fundamentals and Applications*. Cambridge: Cambridge University Press, 2010.